Published in final edited form as:
Integr Biol (Camb). 2012 August ; 4(8): 863–874. doi:10.1039/c2ib00184e.

Mechanism of a flow-gated angiogenesis switch: Early signaling events at cell-matrix and cell-cell junctions

Vernella Vickerman[a] and **Roger D. Kamm**[b]

Roger D. Kamm: rdkamm@mit.edu

[a]Department of Chemical Engineering, Massachusetts Institute of Technology, Cambridge, USA

[b]Departments of Biological and Mechanical Engineering, Massachusetts Institute of Technology, Cambridge, USA. Fax: 617-258-5239; Tel: 617-253-5330

Abstract

A bias towards angiogenesis from the venous circulation has long been known, but its cause remains unclear. Here we explore the possibility that high interstitial pressure in tumors and the resultant net filtration pressure gradient that would induce flow from the interstitium into the venous circulation or lymphatics could also be an important mechanical regulator of angiogenesis. The objective of this study was to test the hypothesis that basal-to-apical (B-A) transendothelial flow promotes angiogenesis and to investigate potential mechanisms. Macro- and microvascular endothelial monolayers were cultured on type I collagen gels in a microfluidic cell culture device and subjected to apical-to-basal (A-B) and B-A transendothelial flows. Samples were perfusion fixed and analyzed for morphological responses, localization and degree of phosphorylation of certain signaling proteins. Application of B-A, but not A-B flow, to cultured endothelial monolayers was found to promote capillary morphogenesis and resulted in distinct localization patterns of VE-Cadherin and increased FAK phosphorylation. These results suggest that B-A flow triggers the transition of vascular endothelial cells from a quiescent to invasive phenotype and that the flow-mediated response involves signaling at cell-cell and cell-matrix interfaces. These results support the hypothesis that transendothelial pressure gradients resulting in B-A flow promotes sprouting angiogenesis and are consistent with early observations that tumor angiogenesis occurs from the venous side of the circulation.

Introduction

Angiogenesis – the formation of new blood vessels from a pre-existing parent vessel – is commonly defined by the imbalance of soluble pro- and anti-angiogenic factors [(1)]. The biochemical regulation which involves the binding of soluble ligands to endothelial cell (EC) surface receptors and subsequent downstream signaling have been painstakingly mapped out by decades of research [(2), (3), (4)]. The *in vivo* endothelial microenvironment however, is a complex integration of both biochemical and biomechanical factors, which

†Electronic Supplementary Information (ESI) available: [Diffusional permeability (P_d), Bead tracer technique for flow rate measurement and endothelial monolayer pressure drop estimation, Time-lapse video microscopy, Transmission electron microscopy and Antibody validation]. See DOI: 10.1039/b000000x/

together promote either a quiescent or angiogenic phenotype. The relative importance of biochemical or biomechanical stimuli in the regulation of endothelial fate and function remains unclear. Nonetheless, it is widely accepted that mechanical forces regulate endothelial cell growth, differentiation, motility, protein synthesis and gene expression [(5)].

Studies of the impact of mechanical stimulation due to fluid flow on cultured endothelial monolayers traditionally focus on the effects of shear stress – an important regulator of vascular tone, homeostasis, inflammatory and immune response. *In vivo,* endothelial cells are subjected to both surface shear flow as well as transendothelial flow - fluid filtration across the endothelium –caused by pressure differentials between luminal/apical and abluminal/basal endothelial surfaces. Apical-to-basal (A-B) transendothelial flow has been shown to inhibit the transmigration of neutrophils across human umbilical vein EC (HUVEC) cultured on polycarbonate filters [(6)], alter EC transport properties [(7)] and influence capillary morphogenesis [(8)] [(9), (10)], although the mechanisms for this remain to be elucidated. Early studies of tumor angiogenesis made the observation that new vessels emerge predominantly from venules [(11)]. However, the direction of transendothelial flow, which is also physiologically relevant, has only recently been investigated in the context of endothelial function or sprouting angiogenesis [(9), (10)].

High interstitial pressure is a hallmark of neoplastic tissue [(12), (13)] and gradients in interstitial pressure are thought to play an important role in a variety of developmental processes [(14)]. With high interstitial pressure induced by the solid tumor, neighboring blood vessels from the lower pressure circulation are potentially affected by the resulting transmural pressure, causing vessel collapse and potentially influencing the rate of transendothelial flow. The resultant net filtration pressure gradient would induce flow from the interstitium into the venous circulation or lymphatics. Endothelial cells lining these vessels would be subjected to transendothelial pressures with higher pressure on the basal-surface compared to the apical surface. Under these conditions basal-to-apical (B-A) transendothelial flow is highly probable.

The objective of this study was to study the role that B-A transendothelial flow exerts on sprouting angiogenesis and to investigate potential mechanisms. In this study, we present evidence of the initial signaling cascade that is initiated by B-A flow and propose links based on our results and previously published work that supports an argument for mechanically-stimulated angiogenesis. We find that FAK-mediated signaling accompanied by extensive remodeling of cell-cell junctions and redistribution of the actin cytoskeleton contributes to the effect of transendothelial flow on vascular sprouting.

Methods

Cell Culture

Human dermal microvascular endothelial cells (HMVEC - cc-2643, LONZA, Walkersville, MD) and human umbilical vein endothelial cells (HUVEC - cc-2617, LONZA) were expanded on collagen-coated flasks in EGM-2MV (cc-3202, LONZA) and EGM-2 (cc-3162, LONZA) medium, respectively. Cells were cultured in a humidified incubator at 37 °C and 5% $C0_2$. All experiments were conducted with passages 4–6 cells. Monolayer

maintenance medium was EGM2MV without hydrocortisone. Experimental medium was maintenance medium supplemented with 20 ng/ml VEGF165 (293-VE-010, R&D Systems Inc., Minneapolis, MN) or VEGF121 (4644-VS-010, R&D Systems Inc.). At this concentration, VEGF was not at sufficient level to induce sprouting under no-flow conditions within 24 hrs.

Microfluidic – based cell culture platform

A microfluidic-based cell culture system with the demonstrated capability of controlling the biochemical environment and flow was used in these studies, as described in detail in [15]. Briefly, the design includes two independent microfluidic channels (240 μm) that are separated by a central region – "gel cage" for housing injectable hydrogels (synthetic peptide, Matrigel, collagen) allowing for simultaneous culture on two-dimensional (2D) surfaces and within three-dimensional (3D) matrices. This geometry permits the establishment of pressure gradients and small interstitial fluid flows through the 3D matrix. The device is fabricated using standard soft lithographic techniques from Polydimethylsiloxane (PDMS – 184 SIL ELAST KIT, Ellsworth Adhesives, Germantown WI), a widely used biocompatible and optically transparent elastomer for microfluidics-based cell culture devices [16]. For a detailed description of device assembly and operation see Vickerman et al 2008 [15]. Interstitial flow (6 μm/s) is established by means of inserting small reservoirs into the inlet and outlet ports of the channels, and regulating and monitoring the relative heights of the liquid columns [15), (17)], thereby allowing both flow rate and pressure drop to be determined by visual inspection (details provided in **Supplementary Information)**.

Imaging

Multiple imaging modalities were used in this study. Phase-contrast (Zeiss Axiovert 200, Carl Zeiss, Germany), epifluoresence (Nikon TE300, Nikon Instruments Inc., NY), confocal (Olympus FluoView 1000, Olympus America, Center Valley, PA and Carl Zeiss 510, Axiovert 200M Laser Scanning Microscope, Carl Zeiss, Germany) and transmission electron microscopy (Model 300, Philips, Eindhoven, The Netherlands) were used to characterize microenvironmental properties, cellular morphology, protein localization and phosphorylation state. EC monolayers grow perpendicular to the imaging plane which readily permits sprout visualization and imaging.

EC monolayer formation and characterization

In the current study, rat tail collagen type I was used as scaffold. Liquid rat tail collagen type I pre-polymer solution (354236, BD Biosciences) was prepared according to product specifications to obtain a final gel concentration of 2.5 mg/ml. Collagen gels and endothelium monolayers were formed in the microfluidic devices as previously described [15]. Briefly, collagen pre-polymer solution at pH=7.4 was microinjected into the gel-cage, sealed with a glass coverslip and polymerized at 37 °C for 30–35 min. Following collagen polymerization, gels were incubated overnight in monolayer maintenance medium. Cell suspension was perfused through one microfluidic channel, device tilted and cells allowed to attach to the collagen gel surface, spread and form a monolayer. Diffusional

permeability, P_d, was measured by monitoring the concentration of fluorescent dextrans introduced via the endothelial-lined channel under steady-state conditions, as described in detail in Supplementary Information. Evaluation of EC expression and localization of adherens and tight junction proteins was done by immunolabeling with purified rabbit polyclonal VE-Cadherin (ALX-210-232-C100, ENZO Life Sciences, Uniondale, PA) and mouse monoclonal ZO-1 (339110, Invitrogen, Chicago, IL) primary antibodies (details below). Labeled monolayers were imaged with a confocal microscope. In separate samples, further ultrastructural characterization was done using transmission electron microscopy (TEM) (details provided in Supplementary Information).

In vitro transendothelial flow angiogenesis assay

Basal-to-apical and A-B trans-endothelial flows were generated by imposing a higher liquid column (typically 80 mm) on the basal or apical surface of the EC monolayer, respectively. The monolayer was perfused with experimental medium for 24 hours whereas non-flow or static conditions were used as control. At the end of an experiment, the monolayer was fixed with 4% paraformaldehyde (PFA), stained with 4′, 6-diamidino-2-phenylindole (DAPI; Sigma-Aldrich, Atlanta, GA) for nuclei and phalloidin (Alexa Fluor 488-phalloidin, Al2379; Invitrogen, Chicago, IL) for actin and stored for further processing. Fixed samples were imaged with a confocal microscope (Olympus FluoView 1000) to generate stacks for further quantification. Length, number of sprouts and total number of cells that invaded in 3D gel were used as simple metric for quantification [18]. For the purpose of quantification, sprouts were defined as capillary-like structures that contained at least one nucleus to distinguish them from invadopodia or filopodia-like membrane projections. Similar experiments were conducted to study the effect of pharmacological inhibition (see details below).

Evaluation of signal transduction at cell-matrix adhesions

Transendothelial flow direction-mediated difference in signalling at cell-matrix adhesion was determined by quantifying levels of phosphorylation of FAK on Tyr 397 compared to total FAK. Antibody pairs were validated (methods described in Supplemental Information) before use for quantification. Endothelial cell monolayers were subjected to A-B, B-A flow or static conditions, perfusion fixed and immunostained with mouse monoclonal anti-FAK (Clone 4.47, Millipore) and rabbit polyclonal anti-*p*-FAK Y397 (ab4803, Abcam Inc.) and appropriate secondary antibodies (detailed below). Samples were also counterstained with DAPI to identify nuclei. Doubly immunolabeled samples were imaged with a confocal microscope (Carl Zeiss 510, Axiovert 200M Laser Scanning Microscope) equipped with a multi-track channel system, to generate stacks (at least 40 slices, 1 μm thick) for p-FAK, FAK and DAPI. ImageJ (U.S. National Institute of Health, Bethesda, MD) [19] was used to quantify florescent intensity for FAK and p-FAK Y397. Average p-FAK/FAK ratio was then calculated for each stack. Average ratios for A-B and B-A flow were normalized by averages from static controls. For quantification, confocal settings were kept the same for all samples. Reported *p-values* were obtained from Student's t-test analysis.

Localization of signaling protein

On the assumption that the morphological changes observed at later times were a consequence of signaling activated much earlier, shorter term experiments were also conducted to study the effects of flow direction on signaling protein localization. HMVEC monolayers were perfused in either B-A or A-B direction for 2 hrs and perfusion fixed while maintaining the initial flow direction. Samples were subsequently immunolabeled (details below) with VE-cadherin antibody (ALX-210-232-C100, ENZO Life Sciences, Uniondale, PA) and imaged with a confocal microscope (Carl Zeiss 510, Axiovert 200M Laser Scanning Microscope). A series of at least 40 optical serial sections were obtained. Each confocal slice yields a cross-sectional view of the monolayer which is formed perpendicular to the optical imaging plane. Enface views showing protein localization on the monolayer was generated from projection of image stacks using LSM Image Browser (Carl Zeiss, Germany) software.

Fluorescent line intensity profiles were obtained for quantitative representation of VE-cadherin distribution. Cross-sectional images of the monolayer were obtained by confocal imaging and processed in ImageJ (U.S. National Institute of Health, Bethesda, MD). Fluorescent intensity was obtained along a horizontal line defined between two adjacent cell-cell junctions. Additional difference in protein distribution due to flow direction was evaluated using kurtosis analysis (20) in ImageJ.

Pharmacological Inhibition

Two sets of pharmacological experiments were conducted: (1) long term, to evaluate the effect of various inhibitors on EC migration or sprouting angiogenesis, and (2) short term, to determine the effect on flow-induced protein localization. For these experiments 3D sprouting assays were repeated in the presence of the following small molecules: Genistein (100 μM; 345834, EMD Chemicals Inc., Gibbstown, NJ), a tyrosine kinase inhibitor [(21)], PP2 (10 μM; 529576, EMD4 Biosciences, San Diego, CA), a Src inhibitor [(22)], Y27632 (50 μM; 688000, EMD4 Biosciences), a Rho-associated kinase (ROCK) inhibitor [(23)], Heparinase III (15 mU/ml; H8891, Sigma-Aldrich, Atlanta, GA), an enzyme that cleaves heparin sulfate of the glycocalyx (24) and L-NAME (100 μM; N5751, Sigma-Aldrich, Atlanta, GA), a nitric oxide synthase (NOS) inhibitor [(25)]. Many dynamic processes and molecular interactions in cells are mediated by protein phosphorylation and Genistein is a widely used tyrosine kinase inhibitor. Rho proteins and their effectors play essential roles in regulating cytoskeletal events critical for cell migration. The main downstream RhoA effector, ROCK, controls actomyosin contractility which is important for 3D cell migration. ROCK inhibition with Y27632 treatment decreases invasive potential of cancer cells [(26)] [(27)]. Furthermore, tumor-derived endothelial cells reportedly record constitutively high levels of ROCK [(28)]. A subset of the pharmacological inhibitors was used to further investigate the effects of inhibition on protein localization. In all studies inhibitors were incubated 2 hours prior to and throughout flow treatment. As before, monolayers were perfusion fixed with 4% PFA, immunostained and imaged by confocal microscopy.

Antibody Labeling and Counterstaining

For antibody labeling, fixed samples were rinsed twice with 1X PBS, permeabilized with 0.1% Triton-X, rinsed twice with 1X PBS and incubated at room temperature for 2 hrs in blocking buffer – 10% BSA in PBS. Following the blocking step, samples were then rinsed once with rinse buffer – 0.5% BSA. Primary and secondary antibodies were diluted in rinse buffer. Blocked samples were incubated with primary antibodies overnight at 4 C. Subsequently, samples were then washed thoroughly with rinse buffer (3-times, 30 min rinse incubation at room temperature) and incubated with secondary antibodies in the dark for 2 hrs. Following indirect antibody labeling, samples were washed thoroughly with 1X PBS and counterstained at the indicated dilution with DAPI (1:1000) to identify nuclei and phalloidin (1:50) to label F-actin. In some cases, fixed and Triton-X treated samples were stained with only DAPI and phalloidin thus the blocking, antibody incubation and associated wash steps were not required.

Results

Formation of a functional EC monolayer

Functional monolayers with barrier function to fluid and macromolecules are vital for establishment of transendothelial pressure gradients and flow. In order to characterize the functionality of the monolayers cultured in our microfluidic device, both the permeability of a 40kDa dextran (typical size of growth factors) and the expression of junction protein were evaluated. EC cultured for 24 hrs on type 1 collagen expressed both tight and adherens junction protein as indicated by immunofluorescence staining for ZO-1 and VE-Cadherin, respectively (Fig. 1). The expression profile is similar to that of ECs cultured on glass (Fig. S1). Ultrastructural analysis of the monolayer from TEM micrographs shows typical junction morphology of extended membrane adhesions (Fig. 1C).

Monolayer functionality was also assessed by testing barrier function of monolayers cultured for 24 hours using a fluorescent 40kDa dextran and computing diffusional permeability. An average P_d value of 9.7×10^{-7} m/s was obtained which is comparable to values reported in the literature for monolayers cultured in vitro [(29)]. Together these results demonstrate that EC formed a functional barrier on the collagen gels within microfluidic device and is capable of supporting transendothelial pressure gradients (see also Discussion).

Switching response evoked by transendothelial flow

Prior studies in our lab have demonstrated the use of our microfluidic-based cell culture device for chemokine or biochemically induced sprouting angiogenesis assays. In the current work, the impact of a biomechanical stimulus –transendothelial flow – on sprouting angiogenesis is investigated. Confluent monolayers of HMVEC were cultured on relatively stiff 3-D collagen gels with minimal (20 ng/ml) VEGF and subjected to control (no-flow), A-B or B-A flow for 24 hrs. B-A flow induced an angiogenic response (Figure 2A, right) while monolayers subjected to A-B or zero flow remained quiescent (Fig. 2A, left). In addition to sprout formation/capillary morphogenesis, B-A flow also induced/triggered invadopodia (extensive and highly branched filopodia-like projections (see movie in

Supplementary Information and sequential images in Fig. 2E for five time points) which are actin rich membrane projections) that extend deep into the 3D gel [9], [10]. Further morphogenesis of these sprout precursors (Fig. 2D, left) result in the formation of sprouts once the nucleus has translocated from the monolayer to the elongating stalk (Fig. 2D, right).

In order to determine if these flow-induced effects were unique to microvascular cells, separate experiments were conducted using HUVECs. Similar to microvascular cells, cells of a macrovascular origin form sprouts in response to B-A flow (see Supplemental Fig. S2.).

Multiple signaling pathways are involved in B-A flow induced sprouting angiogenesis

In order to identify potential signaling pathways that might be involved in B-A transendothelial flow induced angiogenesis, we first used a panel of pharmacological inhibitors to target signaling pathways common to angiogenesis. Protein phosphorylation is a common post-translational modification that affects protein function or state of activation. Tyrosine phosphorylation inhibition, with a natural protein kinase inhibitor, Genistein, blocked invadopodia formation and invasion (Fig. 3), suggesting that B-A flow-induced sprouting angiogenesis is tyrosine phosphorylation-dependent. Treatment with PP2, a specific Src family kinase inhibitor, decreased EC invasion and sprout formation. Rho/ROCK signaling has been reported to be important for angiogenic processes including EC migration, survival and permeability [30]. Inhibition with specific ROCK inhibitor Y27632 blocked B-A transendothelial flow induced EC invasion and sprout formation. Instead, Y27632 treatment resulted in extensive invadopodia devoid of nuclei. These results are consistent with reports that Y27632 blocks VEGF-mediated angiogenesis in retinal explants, EC migration and lumen-containing tube-like structures *in vitro* [30]. Our results demonstrate that invadopodia are necessary for EC invasion and sprout formation but their appearance does not guarantee the formation of sprouts. Transendothelial flow has been reported to upregulate NO production [6]. The NO pathway has been extensively studied in the context of cells exposed to A-B transendothelial flow or transmigration studies. For these reasons, the effect of NO production using the NO inhibitor LNAME was used to investigate the potential role of NO production in B-A flow induced angiogenesis. Consistent with this line of reasoning, NO inhibitor LNAME was also found to reduce B-A mediated EC invasion into collagen gels. The cell surface glycocalyx has been known to mediate shear response in endothelial [31] and vascular smooth muscle cells [32]. To determine the potential role of heparan sulfate proteoglycans (HSPGs), cells were treated with heparinase III and subjected to B-A flow. Similar to other inhibitors, digestion of the glycocalyx reduced B-A flow mediated EC invasion. Collectively, these results from pharmacological inhibition experiments suggest that there are multiple signalling pathways involved in B-A induced sprouting angiogenesis with potential for cross-talks.

B-A flow induced activation of EC occurs via FAK-mediated signaling

Pharmacological studies provided some clues into signaling pathways that might potentially be involved in B-A flow induced sprouting angiogenesis. However further investigation was warranted to identify the initiating event linking flow to signal transduction. To gain deeper insight into the observed switch response we postulated that ECs adherent to a matrix can

sense the direction of transendothelial flow and that the observed difference in migration and sprouting angiogenesis could be attributed to differential activation at adhesion sites. Differential activation via cell-matrix adhesion receptors (e.g. integrins, HSPGs) was by quantifying the ratio of FAK Y397 to total FAK for the two flow directions relative to static control. Transendothelial flow direction induced different levels of FAK-mediated signaling activation as measured by the FAK Y397 to FAK ratio (Fig. 4). Monolayers subjected to B-A flow consistently recorded significantly higher levels of the FAK Y397/FAK ratio compared to those exposed to A-B flow ($p=0.0003$) and compared to controls ($p=0.0005$), whereas A-B flow and control conditions were not significantly different. In Fig. 4D(right), the increase in pFAK at 6 hour was due to relative decrease for A-B flow (the error bar was left out intentionally due to limited data at this time point). These results demonstrate that flow direction differentially affects FAK-mediated signaling.

Transendothelial flow direction differentially affects VE-cadherin localization

Since signal transmitted via cell-matrix receptor, for example through integrins which has been shown to regulate junctional remodeling [33], the effect of flow direction on endothelial cell-cell junction protein distribution was assessed. Confluent monolayers were perfused for 2 hrs in either apical-to-basal or B-A flow direction, perfusion fixed and stained for junction protein to capture early signs of differential protein distribution (Fig. 5). B-A flow caused delocalization of VE-cadherin from cell-cell junctions, while samples subjected to A-B flow retained well-defined junctional labeling. Compared to static controls there was no noticeable change in VE-cadherin localization that could be attributed to A-B flow. For the case of A-B flow, fluorescent intensity line profiles across the cell (Fig. 5C) show distinct peaks and valleys corresponding to high and low VE-cadherin expression at cell-cell junctions and in the cytoplasm, respectively. A similar analysis for monolayers subjected to B-A flow yields, by comparison, a relatively uniform profile. Furthermore, kurtosis analysis confirms the visually observed difference in VE-Cadherin protein localization pattern as a function of transendothelial flow direction. These results demonstrate that flow direction differentially affects adherens junction remodeling and confirms the plasticity of cell-cell contacts, an important prerequisite for migration and angiogenesis.

Transendothelial flow direction differentially affects actin cytoskeletal organization

Because forces acting on focal adhesions often lead to recruitment or rearrangement of various intracellular proteins including actin [34], [35], [36], we investigated the effect of transendothelial flow direction on actin distribution. In addition, since cell-cell junctions are mechanically coupled to actin cytoskeleton, we suspected that reorganization of VE-cadherin complexes might also result in remodeling of the actin cytoskeleton. Transendothelial flow direction exerted a strong influence on the intracellular distribution of F-actin as revealed by confocal sections of phalloidin stained monolayers [Fig. 6]. Monolayers subjected to A-B flow exhibited dense actin labeling at cell-cell contacts, whereas monolayers exposed to B-A flow exhibited a more diffuse/disorganized staining pattern. In addition B-A flow induced clustering of actin near the basal surface [Fig. 6D] from which “hair-like” structures emerged [Fig. 6D (ii)], at the tips or filopodia/invadapodia [Fig. 6D (iii)] and the base of newly forming sprouts [Fig. 6D (i)].

VE-Cadherin delocalization is mediated by Src

Src is important in mediating communication between focal adhesions and cell-cell junctions [37], and has been implicated in angiogenesis in vivo and in vitro [38]. Our results show clustering of phosphorylated Src at locations in monolayers from which sprouts emerged [Fig. 7]. Src is reportedly a key mediator in signal transduction between integrin-mediated adhesions and cadherin mediated cell-cell contacts [37]. Furthermore upon integrin activation, Src associates with FAK in focal complexes and VE-cadherin is known to possess a Src phosphorylation site on Tyr 658 [39], [40]. We therefore wanted to determine whether B-A flow induced VE-cadherin redistribution at cell-cell contact was mediated by Src. Treating monolayers with PP2 prior to and during the application of B-A flow, we found that this Src-family kinase specific inhibitor was able to substantially reduce B-A flow induced VE-cadherin delocalization, demonstrating that B-A flow induced VE-cadherin delocalization at cell-cell junction is mediated by Src.

Conclusions

Cells are continuously experiencing external mechanical perturbations within their environment and mechanical forces play an important role in physiological as well pathological conditions. Of particular interest is the role that mechanical forces play in the tumor microenvironment. Much of the work published on endothelial mechanotransduction addresses cardiovascular diseases while tumor vascularization studies typically focus on the chemo-regulation in the recruitment of new blood vessels. Here we explore flow-mediated regulation of angiogenesis that could potentially occur in a tumor environment due high interstitial fluid pressure (41), (12), (42) and lower microvascular pressure compare to normal tissues (12) and demonstrate that sprouting angiogenesis can be promoted by B-A transendothelial flow through a process that is mediated by FAK at the cell-matrix interface. We postulate that B-A transendothelial flow could occur in neoplastic tissues. In further support of this line of reasoning, robust angiogenesis is observed at the tumor margin/periphery (43) where there would be high gradients in pressure (42). The tumor microenvironment is mechanically dynamic and mechanical stress due to high interstitial pressures which is known to impact tumor cell function (44), (45) may be an important factor in regulating endothelial function and the initiation of angiogenic sprouts.

Flow direction acts as an angiogenic switch

We investigated the effect of transendothelial flow direction on sprouting angiogenesis and observed a switch-like response in which B-A flow promotes angiogenesis but the reverse flow direction, A-B, did not. Our results therefore suggest that transendothelial flow direction acts as an *angiogenic switch*. B-A flow promotes angiogenesis in micro- and macro- vascular endothelial cells – defining an angiogenic ON state while the alternate flow direction – apical-to-basal – maintains the OFF state. This behavior is consistent with the early observation that neovascularization in tumors originate from venules and post-capillary venules [11].

EC activation is due to mechanical stimulation

The observed angiogenic response could be due to either biochemical or biomechanical stimuli. We first explored the hypothesis that a migratory stimulus could arise due to concentration polarization of soluble or matrix-bound growth factors (e.g. VEGF) arising from B-A flow in combination with the low permeability of the endothelial monolayer. Experiments at saturation levels of VEGF165 and VEGF121 (the non-binding isoform) (results not shown) confirmed that the influence of flow direction was unaltered. Furthermore, intuition, confirmed by numerical simulation, tells us that although B-A flow could lead to higher concentrations at the basal membrane, it would also produce a gradient that would not be favourable for sprouting. A favourable gradient would produce lower concentration near the basal membrane and gradually higher concentration as you move away from the basal surface across the length of the gel. Here, the endothelial monolayer selectivity to macromolecule for example, VEGF could potentially cause a “pile up” at the basal surface even with an initially uniform concentration throughout the device and equal concentration in reservoirs. However, concentration polarization during B-A flow would produce a gradient of the opposite sign, meaning that sprouts would be growing in the direction of reducing concentration. Thus, although we cannot completely rule out the possibility that biochemical effects contribute to our observations; this evidence suggests that factors other than biochemical gradients are responsible.

B-A Flow increases FAK-mediated signaling at cell-matrix adhesions

Based on the low hydraulic permeability of the endothelial monolayer, a simple force balance dictates that the pressure difference associated with B-A flow would give rise to a net force acting to lift the cells off the hydrogel surface. Since separation was not observed, presumably the cell matrix adhesions, $\alpha_1\beta_1$ or $\alpha_2\beta_1$ integrins in the case of type I collagen, must be capable of supporting the force arising from this pressure drop. Conversely, in A-B flow, the cell can be supported by direct physical contact with the gel; to the extent that the cell adhesion receptor-collagen bonds support the load, it would be compressive rather than tensile. It is well established that integrins transduce signals from the extracellular matrix [(46)], and that mechanical force leads to integrin activation [(47)] resulting from integrin conformational change [(48)] or clustering [(49)] [(50)]. While there is insufficient evidence to irrefutably name the specific cell-matrix adhesion mechanosensor, based on evidence in the literature and models describing the signalling events following integrin activation it is tempting to speculate that the observed difference due to flow direction is integrin-mediated. It is widely accepted that integrin activation leads subsequently to phosphorylation of Tyr 397 in focal adhesion kinase (FAK). Nevertheless, we cannot completely rule out potential contributions due to non-integrin mediated signalling. Our observations that B-A flow induces a significant increase in the ratio of p-FAK to total FAK when compared to A-B or static conditions therefore supports the role of FAK-mediated signalling in the cellular response due to increased autophosphorylation and potential integrin activation. A recent study by Shi et al., [(32)], reports on FAK-mediated signalling downstream of HSPGs induced by interstitial flow for vascular smooth muscle cells (SMCs) suspended in collagen gel. Here they propose a cooperative interaction between integrin and HSPGs with the latter being the main signal transducer. A potential role of HSPGs is also plausible in our current study on the basis of the observed inhibitory effect of heparinase treatment on B-A flow induced cell

invasion. Unlike in our current study, Shi et al., [32] did not observe changes in FAK phosphorylation on Tyr 397, instead a flow mediated difference was observed at Tyr 925. Due to differences in cell type (SMCs vs. EC), seeding configuration (3D suspended cells vs. monolayer) that might affect the distribution of HSPGs on the cell surface and other differences in experimental methods it is difficult to reconcile the differences in FAK-mediated signalling and subsequent conceptual models. Nevertheless, crosstalk between signalling pathways downstream of individual mechanosensors in general is highly probable. Furthermore given the molecular complexity and diversity at these sites of cell-matrix contacts cooperative interactions are foreseeable which presents a challenge in identifying individual contributors. Consequently, further investigation is necessary to identify potential mechanosensor(s) and to determine the involvement of integrins, HSPGs or both in the current model. Nevertheless we cannot conclude whether the glycocalyx and integrin act independently or the nature of any potential interaction.

We postulate that at the molecular level, B-A flow produces tension at the site of cell-matrix adhesion and subsequent activation as measured by FAK Y397 levels. Src, which translocates to cell-matrix adhesions following integrin activation, subsequently becomes activated. Following this initial event Src further phosphorylates FAK on multiple other sites including Tyr 576 and Tyr 577 in the activation loop, which promotes optimal FAK activity [39]. We propose that this is the major difference between flow directions that results in the observed angiogenic response.

B-A flow induced VE-Cadherin delocalization and angiogenesis are mediated by Src

VE-Cadherin engages in homophilic interactions between neighboring cells and its presence at cell-cell junctions is typical of a quiescent endothelial phenotype. We demonstrate here that B-A flow promotes delocalization of VE-cadherin from cell-cell junctions, while static or apical-to-basal flow does not. While this could be a direct consequence of forces acting at the cell-cell junction, we postulated that this junctional remodeling is due instead to signaling initiated by integrin activation. VE-cadherin intercellular adhesive activity is regulated by cytoplasmic signaling events involving catenins, which can be abolished by tyrosine phosphorylation of both catenin and VE-cadherin. Disruption of cadherin-catenin complexes causes the destabilization of intercellular junctions [51]. Remodeling of adherens junction can occur due to VE-cadherin internalization, enzymatic cleavage or kinase phosphorylation. Tyrosine phosphorylation of Y658 or Y731 on VE-cadherin prevents the binding of p120- and β-catenin, respectively [52]. VE-cadherin retention at adherens junctions requires association with p120 [53]. B-A flow can therefore initiate a signaling cascade that causes disruption of adhesion complexes and subsequently delocalization of VE-cadherin. Furthermore, VE-cadherin is a substrate for Src [52] and is phosphorylated on Y685 [40]. Additionally, phosphorylation of VE-cadherin is inhibited in Src-deficient mice [54]. For Src to function, the Src kinase domain must be unmasked. Src is activated by both growth-factor initiated signals [55] and those of a mechanical origin [47]. VE-Cadherin complex disruption has been shown to enhance angiogenesis [56]. While the detailed events leading to Src activation and subsequent association with VE-cadherin are beyond the scope of this paper, presumably, Src activation follows from B-A flow induced integrin activation. We also showed in pharmacological studies that VE-cadherin delocalization is Src-

mediated; inhibition with PP2 blocks VE-cadherin delocalization during B-A flow. Based on these findings we infer that VE-cadherin delocalization from intercellular junctions was likely due to phosphorylation of VE-cadherin which was mediated by Src and downstream of integrin activation.

Reorganization of actin cytoskeleton by transendothelial flow

The cytoskeleton is a key player in mechanotransduction [57] and invasive cell migration, which involves dynamic remodeling of actin cytoskeleton, is essential for angiogenesis. FAK promotes cell motility by activating regulators of cytoskeletal dynamics (e.g. Rac1) [58] and the intercellular adhesion complex is mechanically coupled to the actin cytoskeleton. It therefore follows that reorganization of VE-cadherin would affect distribution of actin at junctions. Direct evidence of cortical actin remodeling in the endothelial monolayer during sprouting angiogenesis is not available. Wang and colleagues reported VE-cadherin and actin remodeling when cultured cells were treated with ECM coated beads [33]. Moreover, parallels can be drawn between sprouting angiogenesis and epithelial-to-mesenchymal transition (EMT) where cells transition from a stable endothelial (angiogenesis) or epithelial (see [59] for review) monolayer to acquire a migratory phenotype. Remodeling of cortical actin to actin stress fibers is a distinct feature of migratory mesenchymal cells [60]. Epithelial cells exhibit cortical actin while transformed mesenchymal cells do not [61]. Moreover, Src kinase activity is required for protrusion dynamics specifically; phosphorylation of FAK on Tyr 925 is directly mediated by Src and is necessary for the dynamic regulation of matrix adhesion during cell migration [62].

Force estimates acting on the monolayer

Numerous studies have investigated the forces necessary to elicit a mechanoresponse, so it is useful to compare the levels of force acting on the monolayer to those associated with other mechanotransduction phenomena. While it is difficult to determine the pressure drop across the monolayer as distinct from that across the gel-monolayer combination, based on a comparison of the flow through the matrix with and without a monolayer present, we estimate that under our experimental conditions, the monolayer supports a pressure of ~15 Pa. Using this value in combination with an estimated cell area of ~500 μm^2, we arrive at a value of ~7 nN supported by each cell; this level of force is well in excess of that required by endothelial cell activation by shear stress (~0.5 nN) [63, 64] or by direct application of force by pulling on cell-tethered beads (~1.0 nN) [65]. Therefore, in terms of force magnitude alone, it is not surprising that B-A flow activates mechanotransduction pathways.

Summary Proposed Model

Collectively, these results suggest that B-A flow triggers the transition of vascular endothelial cells from a quiescent to a migratory phenotype. We present evidence of a signaling cascade that is initiated at focal adhesions and subsequently transduced across the plasma membrane prompting changes at cell-cell junctions and within the actin cytoskeleton. We propose that B-A flow produces mechanical stress at cell-matrix adhesions, which leads to FAK-mediated signaling, Src-mediated cell-cell junction remodeling and delocalization of VE-cadherin and cytoskeleton reorganization which promotes a transition from a quiescent to an invasive/angiogenic phenotype. Multiple pro-

angiogenic signaling cascades follow FAK activation and VE-cadherin remodeling which would trigger endothelial cell invasion and angiogenesis. Furthermore, Src-induced deregulation at cadherin junctions in cancer cells require integrin signaling [37], and invadopodia dynamics during migration requires Src-specific phosphorylation of FAK [62].

In vivo, new blood vessels predominantly emerge from postcapillary venules which is the lower pressure side of the circulation and would be more susceptible to B-A transendothelial flows in a high pressure tumor environment. Following this line of reasoning, B-A flow could also contribute to tumor angiogenesis. It is intriguing that similar results can be captured in our microfluidic system, which opens the opportunity for future investigation of angiogenesis where both biochemical and biomechanical environment is recapitulated.

Supplementary Material

Refer to Web version on PubMed Central for supplementary material.

Acknowledgments

The authors thank Haiyan Gong for TEM imaging and use of their confocal imaging facility. We thank Choong Kim for help with3D graphics and Carlos Semino for helpful discussion. This work was supported by funding from NIBIB (EB003805) NSF SCT (CBET-0939511) and NSF-EFRI (0735997).

References

1. Carmeliet P. Nat Med. 2003; 9:653–660. [PubMed: 12778163]
2. Folkman J. Nat Med. 1995; 1:27–31. [PubMed: 7584949]
3. Risau W. Nature. 1997; 386:671–674. [PubMed: 9109485]
4. Carmeliet P, Jain RK. Nature. 2011; 473:298–307. [PubMed: 21593862]
5. Chien S, Li S, Shyy JYJ. Hypertension. 1998; 31:162–169. [PubMed: 9453297]
6. Burns AR, Zheng Z, Soubra SH, Chen J, Rumbaut RE. Am J Physiol Heart Circ Physiol. 2007; 293:H2904–H2910. [PubMed: 17720767]
7. Kim MH, Harris NR, Tarbell JM. Am J Physiol Heart Circ Physiol. 2005; 289:H2551–H2558. [PubMed: 16113077]
8. Semino CE, Kamm RD, Lauffenburger DA. Exp Cell Res. 2006; 312:289–298. [PubMed: 16337626]
9. Vickerman, V.; Kamm, RD. Singapore; World Congress of Biomechanics; 2010.
10. Song JW, Munn LL. Proc Natl Acad Sci U S A. 2011; 108:15342–15347. [PubMed: 21876168]
11. Ausprunk DH, Folkman J. Microvasc Res. 1977; 14:53–65. [PubMed: 895546]
12. Jain RK. Cancer Res. 1987; 47:3039–3051. [PubMed: 3555767]
13. Heldin CH, Rubin K, Pietras K, Ostman A. Nat Rev Cancer. 2004; 4:806–813. [PubMed: 15510161]
14. Rutkowski JM, Swartz MA. Trends Cell Biol. 2007; 17:4450.
15. Vickerman V, Blundo J, Chung S, Kamm R. Lab Chip. 2008; 8:1468–1477. [PubMed: 18818801]
16. Duffy DC, Mcdonald JC, Schueller OJ, Whitesides GM. Anal Chem. 1998; 70:4974–4984. [PubMed: 21644679]
17. Sudo R, Chung S, Zervantonakis IK, Vickerman V, Toshimitsu Y, Griffith LG, Kamm RD. FASEB J. 2009; 23:2155–2164. [PubMed: 19246488]
18. Das A, Lauffenburger D, Asada H, Kamm R. Cell Mol Bioeng. 3:345–360.
19. Abràmoff MD, Magalhães PJ, Ram SJ. Biophotonics Int. 2004; 11:36–42.

20. Thi MM, Tarbell JM, Weinbaum S, Spray DC. Proc Natl Acad Sci USA. 2004; 101:16483–8. [PubMed: 15545600]
21. Akiyama T, Ishida J, Nakagawa S, Ogawara H, Watanabe S, Itoh N, Shibuya M, Fukami Y. J Biol Chem. 1987; 262:5592–5595. [PubMed: 3106339]
22. Hanke JH, Gardner JP, Dow RL, Changelian PS, Brissette WH, Weringer EJ, Pollok BA, Connelly PA. J Biol Chem. 1996; 271:695–701. [PubMed: 8557675]
23. Uehata M, Ishizaki T, Satoh H, Ono T, Kawahara T, Morishita T, Tamakawa H, Yamagami K, Inui J, Maekawa M, Narumiya S. Nature. 1997; 389:990–994. [PubMed: 9353125]
24. Ainslie KM, Garanich JS, Dull RO, Tarbell JM. J Appl Physiol. 2005; 98:242–9. [PubMed: 15322072]
25. Rees DD, Palmer RM, Schultz R, Hodson HF, Moncada S. Br J Pharmacol. 1990; 101:746–752. [PubMed: 1706208]
26. Wyckoff JB, Pinner SE, Gschmeissner S, Condeelis JS, Sahai E. Curr Biol. 2006; 16:1515–1523. [PubMed: 16890527]
27. Routhier A, Astuccio M, Lahey D, Monfredo N, Johnson A, Callahan W, Partington A, Fellows K, Ouellette L, Zhidro S, Goodrow C, Smith A, Sullivan K, Simone P, Le L, Vezuli B, Zohni M, West E, Gleason D, Bryan B. Oncol Rep. 2010; 23:861–867. [PubMed: 20127030]
28. Ghosh K, Thodeti CK, Dudley AC, Mammoto A, Klagsbrun M, Ingber DE. Proc Natl Acad Sci U S A. 2008:11305–11310. [PubMed: 18685096]
29. Chang YS, Munn LL, Hillsley MV, Dull RO, Yuan J, Lakshminarayanan S, Gardner TW, Jain RK, Tarbel JM. Microvasc Res. 2000; 59:265–277. [PubMed: 10684732]
30. Bryan BA, Dennstedt E, Mitchell DC, Walshe TE, Noma K, Loureiro R, Saint-Geniez M, Campaigniac JP, Liao JK, D'Amore PA. FASEB J. 2010; 24:3186–3195. [PubMed: 20400538]
31. Florian JA, Kosky JR, Ainslie K, Pang Z, Dull RO, Tarbell JM. Circ Res. 2003; 93:136–42.
32. Shi ZD, Wang H, Tarbell JM. PLoS One. 2011; 6:15956.
33. Wang Y, Jin G, Miao H, Li JY, Usami S, Chien S. Proc Natl Acad Sci U S A. 2006; 103:1774–1779. [PubMed: 16446427]
34. Galbraith CG, Yamada KM, Sheetz MP. J Cell Biol. 2002; 159:695–705. [PubMed: 12446745]
35. Icard-Arcizet D, Cardoso O, Richert A, Hénon S. Biophys J. 2008; 94:2906–2913. [PubMed: 18178644]
36. Ueki Y, Sakamoto N, Sato M. Open Biomed Eng J. 2010; 4:129–134. [PubMed: 21611138]
37. Avizienyte E, Wyke AW, Jones RJ, Mclean GW, Westhoff MA, Brunton VG, Frame MC. Nat Cell Biol. 2002; 4:632–638. [PubMed: 12134161]
38. Kilarski WW, Jura N, Gerwins P. Exp Cell Res. 2003; 291:70–82. [PubMed: 14597409]
39. Ruest PJ, Roy S, Shi E, Mernaugh RL, Hanks SK. Cell Growth Differ. 2000; 11:41–48. [PubMed: 10672902]
40. Wallez Y, Cand F, Cruzalequi F, Wernstedt C, Souchelnytskyi S, Vilgrain I, Huber P. Oncogene. 2007; 26:1067–1077. [PubMed: 16909109]
41. Heldin CH, Rubin K, Pietras K, Ostman A. Nat Rev Cancer. 2004; 4:806–13. [PubMed: 15510161]
42. Boucher Y, Baxter LT, Jain RK. Cancer Res. 1990; 50:4478–84. [PubMed: 2369726]
43. Holash J, Maisonpierre PC, Compton D, Boland P, Alexander CR, Zagzag D, Yancopoulos GD, Wiegand SJ. Science. 1999; 284:1994–8. [PubMed: 10373119]
44. Hofmann M, Gushel M, Bernd A, Bereiter-Hahn J, Kaufmann R, Tandi C, Wiig H, Kippenberger S. Neoplasia. 2006; 8:89–95. [PubMed: 16611401]
45. Raju B, Haug SR, Ibrahim SO, Heyeraas KJ. J Oral Pathol Med. 2008; 37:137–44. [PubMed: 18251937]
46. Juliano RL, Haskill S. J Cell Biol. 1993; 120:577–585. [PubMed: 8381117]
47. Wang Y, Botvinick EL, Zhao Y, Berns MW, Usami S, Tsien RY, Chien S. Nature. 2005; 434:1040–1045. [PubMed: 15846350]
48. Katsumi A, Naoe T, Matsushita T, Kaibuchi K, Schwartz MA. J Biol Chem. 2005; 280:16546–16549. [PubMed: 15760908]

49. Schaller MD, Borgman CA, Cobb BS, Vines RR, Reynolds AB, Parsons JT. Proc Natl Acad Sci U S A. 1992; 89:5192–5196. [PubMed: 1594631]
50. Kornberg L, Earp HS, Parsons JT, Schaller M, Juliano RL. J Biol Chem. 1992; 267:23439–23442. [PubMed: 1429685]
51. Cavallaro U, Christofori G. Nat Rev Cancer. 2004; 4:118–132. [PubMed: 14964308]
52. Potter MD, Barbero S, Cheresh DA. J Biol Chem. 2005; 36:31906–31912. [PubMed: 16027153]
53. Hatanaka K, Simons M, Murakami M. Am J Physiol Heart Circ Physiol. 2011; 300:H162–H172. [PubMed: 21037229]
54. Weis SM, Cheresh DA. Nature. 2005; 437:497–504. [PubMed: 16177780]
55. Van der Heyden MA, Oude Weernink PA, Oirschot BA, Van Bergen en Henegouwen PM, Boonstra J, Rijksen G. Biochim Biophys Acta. 1997; 1359:211–221. [PubMed: 9434127]
56. Nagashima H, Okada M, Hidai C, Hosoda S, Kasanuki H, Kawana M. Heart Vessels. 1997; (Suppl 12):110–112. [PubMed: 9476558]
57. Alenghat FJ, Ingber DE. Sci STKE. 2002; 2002:pe6. [PubMed: 11842240]
58. Brakebusch C, Bouvard D, Stanchi F, Sakai T, Fässler R. J Clin Invest. 2002; 109:999–1006. [PubMed: 11956235]
59. Thiery JP. Nat Rev Cancer. 2002; 2:442–454. [PubMed: 12189386]
60. Boland S, Boisvieux-Ulrich E, Houcine O, Baeza-Squiban A, Pouchelet M, Schoëvaërt D, Marano F. J Cell Sci. 1996; 109:2207–2219. [PubMed: 8886972]
61. Das S, Becker BN, Hoffmann FM, Mertz JE. BMC Cell Biol. 2009; 10:94. [PubMed: 20025777]
62. Brunton VG, Avizienyte E, Fincham VJ, Serrels B, Metcalf CA 3rd, Sawyer TK, Frame MC. Cancer Res. 2005; 65:1335–1342. [PubMed: 15735019]
63. Davies PF. Physiol Rev. 1995; 75:519–560. [PubMed: 7624393]
64. Chiu JJ, Chien S. Physiol Rev. 2011; 91:327–387. [PubMed: 21248169]
65. Mack PJ, Kaazempur-Mofrad MR, Karcher H, Lee RT, Kamm RD. Am J Physiol Cell Physiol. 2004; 287:C954–C962. [PubMed: 15189816]

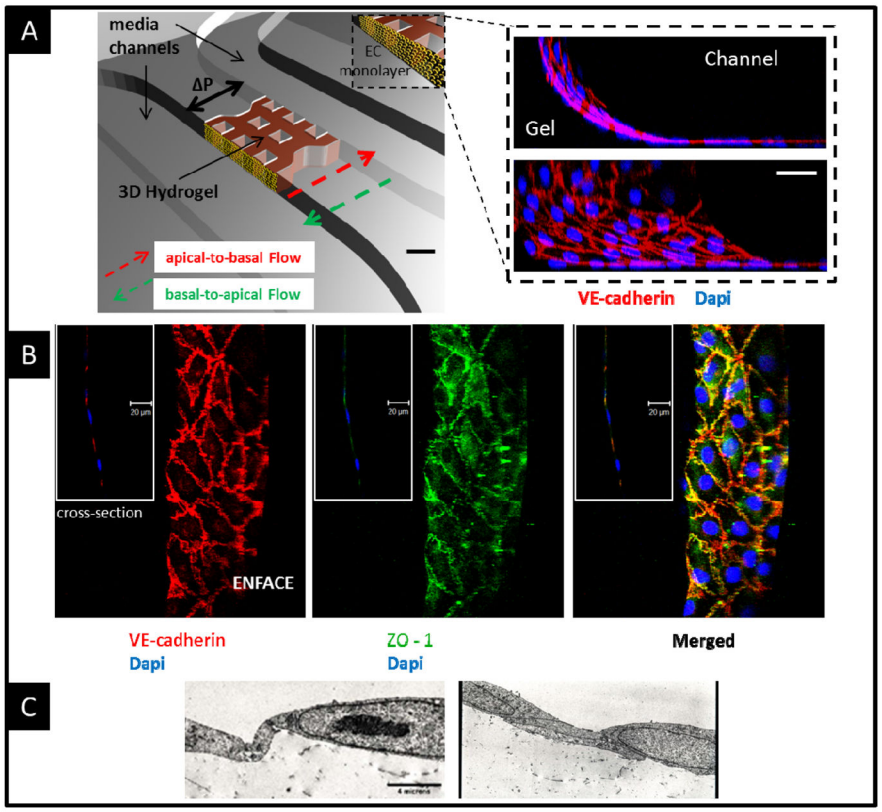

Figure 1.

Microfluidic-based 3D cell culture system for studies of the effects of transendothelial flow on sprouting angiogenesis from an endothelial monolayer. (A) Layout of microfluidic-based 3D cell culture system. Design features include “gel-cage” loaded with collagen gel (pink), an array of pillars (white squares) for mechanically supporting the gel and two parallel fluidic channels (denoted apical- and basal at pressures P_1 and P_2, respectively). Single cell suspension is perfused through the apical channel and an endothelial monolayer grows to confluence. (Dashed arrows denote direction of flow). Transendothelial flow is established in either A-B (red) or B-A (green) direction by applying a pressure gradient across the gel-cage Scale bar 500 μm. (B) Confocal images of endothelial monolayer showing coverage on gel and channel surfaces, immunostained with anti-VE-cadherin (Red) and nuclei (Blue). To confirm that EC form physiologically relevant monolayers the quality of cell-cell junction was evaluated. (B) Localization of tight junction and adherens junction proteins was analyzed by confocal microscopy (Magnification 40x). En face view of doublylabeled monolayer (i) VE-Cadherin, (ii) ZO-1 and (iii) merged images indicating colocalization at cell-cell contacts. Inset shows cross-sectional views. (C) Ultrastructure of cell-cell junction of monolayer cultured in the device was analyzed by transmission electron microscopy (TEM). Micrograph of EC cell-cell contact shows typical junction morphology.

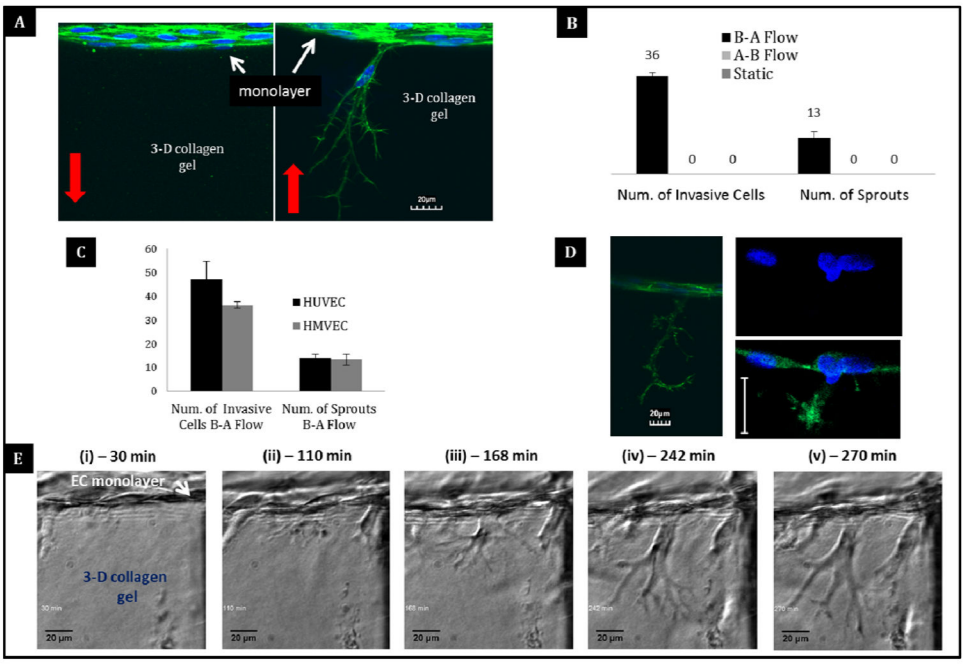

Figure 2.

Transendothelial flow direction modulates EC monolayer phenotype (Red arrow indicates flow direction). HMVECs are cultured on rat tail collagen type I gels and subjected to B-A, A-B flow and static control. (A) Fluorescent micrograph of HMVEC monolayer subjected to A-B (LEFT) and B-A (RIGHT) transendothelial flow (green-actin cytoskeleton, blue-nucleus). Scale bar = 20 μm. (B) Quantification of the asymmetric response that is observed. The average number of cells that have migrated into the collagen gel as well as average number of sprouts per device is reported. (Note: Some cells also migrate as single cells and are not considered as sprouts). (C) Comparison of B-A induced sprouting in HUVECs (macrovascular EC) and HMVECs (microvascular EC).) (D) Confocal image of invadopodia and nucleus deformation during the formation of true spouts. (E) Time-lapse images from video micrograph during B-A flow induced sprouting angiogenesis. Endothelial cells project invadopodia in response to B-A flow initiation and subsequently invade the underlying collagen gel to form sprouts. Scale bar = 20μm

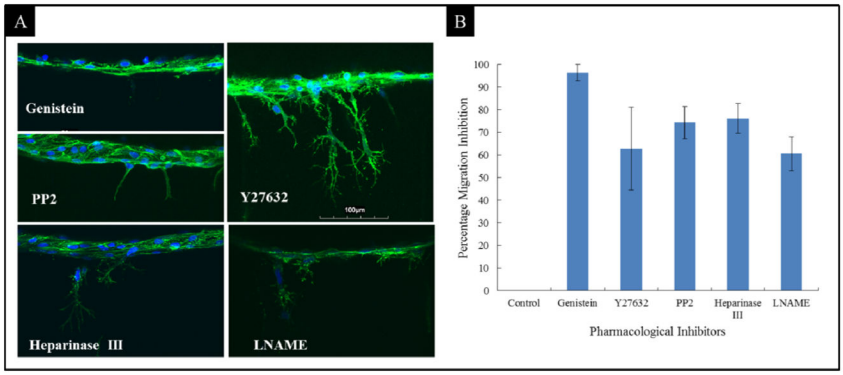

Figure 3.

Inhibition of B-A flow induced angiogenesis by small molecule pharmacological inhibitors. Multiple potential signaling pathways are involved in B-A flow induced sprouting angiogenesis. EC monolayers were generated as described in Methods. Monolayers were incubated for 2 hours with experimental medium containing pharmacological inhibitors prior to and during B-A perfusion. Monolayers were perfused for a total of 24 hours, fixed with 4% PFA and stained for actin and nuclei with phalloidin and DAPI respectively. Samples were subsequently imaged and the degree of inhibition quantified. (A) Panel of representative confocal micrographs of monolayers subjected to B-A flow in the presence of inhibitors for Rho kinase (Y27633, 50μM), Tyrosine phosphorylation (Genistein, 100μM), Src kinase (PP2, 10μM), Nitric oxide (LNAME, 100μM)and enzyme specific to heparan sulfate –cell glycocalyx component (Heparinase III, 15 mU/ml). (B) Quantification of the inhibitory effects of pharmacological inhibitors.

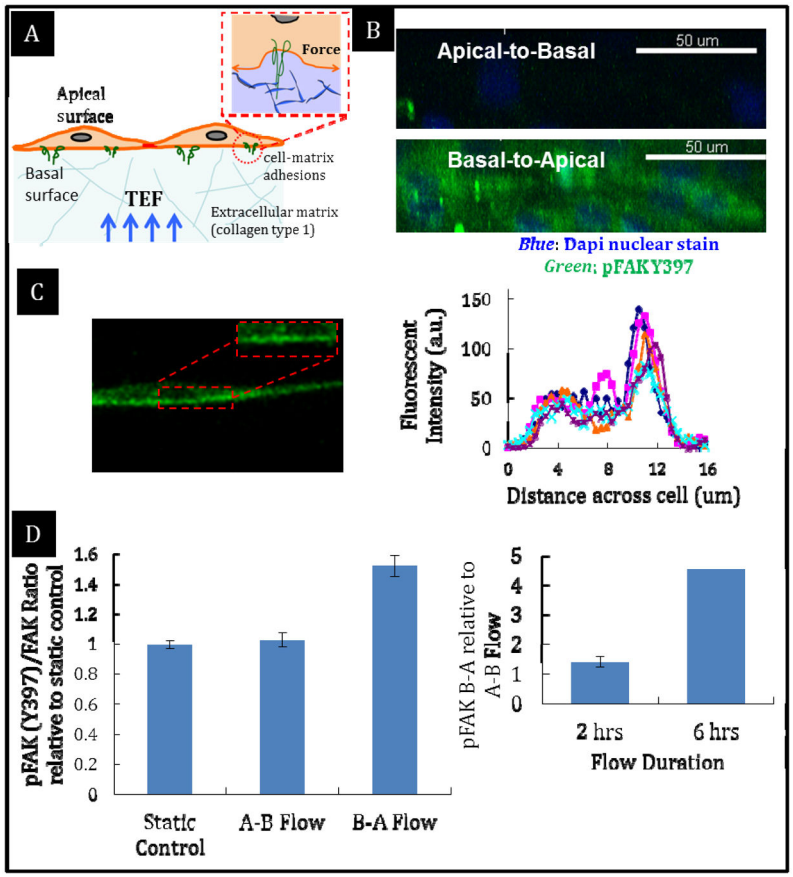

Figure 4.

B-A flow induced activation of ECs occur via FAK-mediated signaling. (A) Schematic of B-A flow induced forces focused at cell-matrix adhesions. EC monolayers were subjected to 2 and6 hrs of static, apical-to-basal and B-A flow conditions. Fixed samples were labeled with anti-FAK and p-FAK Y397 antibodies. (B) En face view of monolayer subjected to apical-to-basal (TOP) and B-A (BOTTOM) transendothelial flows labeled with p-FAK Y397 antibody. (C) Confocal image showing cross-sectional view of EC monolayer subjected to B-A flow and labeled with p-FAK Y397 antibody (LEFT) and fluorescent line intensity profile (RIGHT) from apical to basal cell surface showing asymmetry of p-FAK Y397 distribution towards cell-matrix interface. To evaluate flow direction-dependent changes at cell-matrix adhesions the ratio of p-FAK to total FAK was obtained for monolayers under static, A-B and B-A flow treatments. (D) (LEFT) Quantification of pFAK Y397/FAK ratio. Values are reported relative to static controls. B-A flow samples are significantly different compared to apical-to-basal and static treatments (p-values 0.0003 and 0.0005 respectively). No significant difference between static and apical-to-basal treatment (p value 0.44). (RIGHT) Relative levels of p-FAK Y397 at 2 and 6 hours.

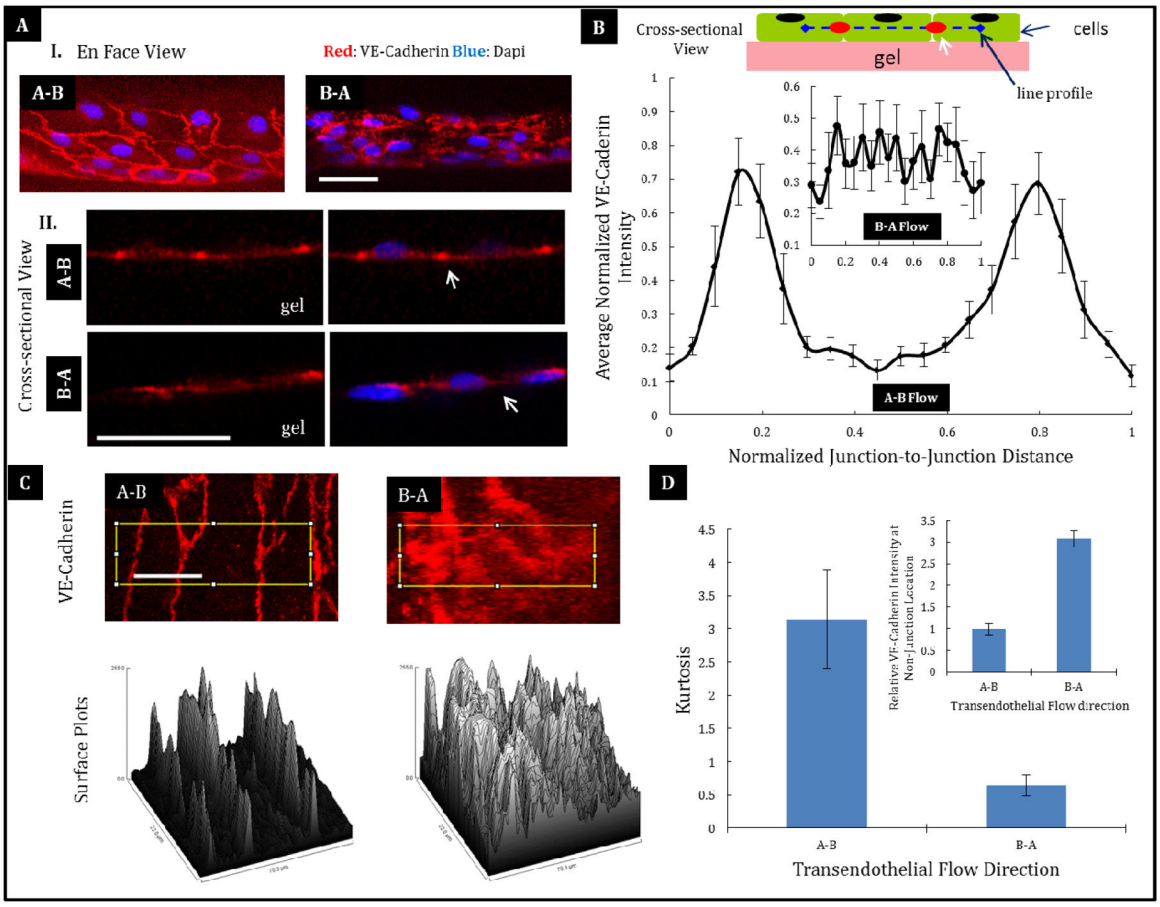

Figure 5.

B-A flow induces delocalization of VE-Cadherin. Functional monolayers were generated as described in Methods. HMVEC monolayer was subjected to 2 hrs static, A-B and B-A flow treatment. The effect of flow direction on protein remodelling at cell-cell junctions was evaluated using confocal microscopy of samples immunolabeled with VE-Cadherin antibody. (A-I.) Enface view of monolayer subjected to A-B (Left) or B-A (Right) transendothelial flow. (A-II.) Cross-sectional view for A-B (Top row) and B-A (Bottom row) treatment. Scale bar: 50 μm (B) (TOP) Schematic of the procedure used for obtaining VE-cadherin intensity profile from images with a cross-sectional view of the monolayer. (Bottom) Fluorescent intensitylines profile across cell for A-B and (Inset) B-A flow. (C) Enface views of monolayers and corresponding surface plotsfor boxed region for A-B (Bottom, left) and (B-A, Bottom, right). Scale bar: 25 μm (D) Kurtosis analysis of VE-Cadherin distribution, showing differences as function of flow direction. (Inset) Quantification of VE-Cadherin intensity, relative to background, at cell interior or non-junctional locations for A-B and B-A flow treatment.

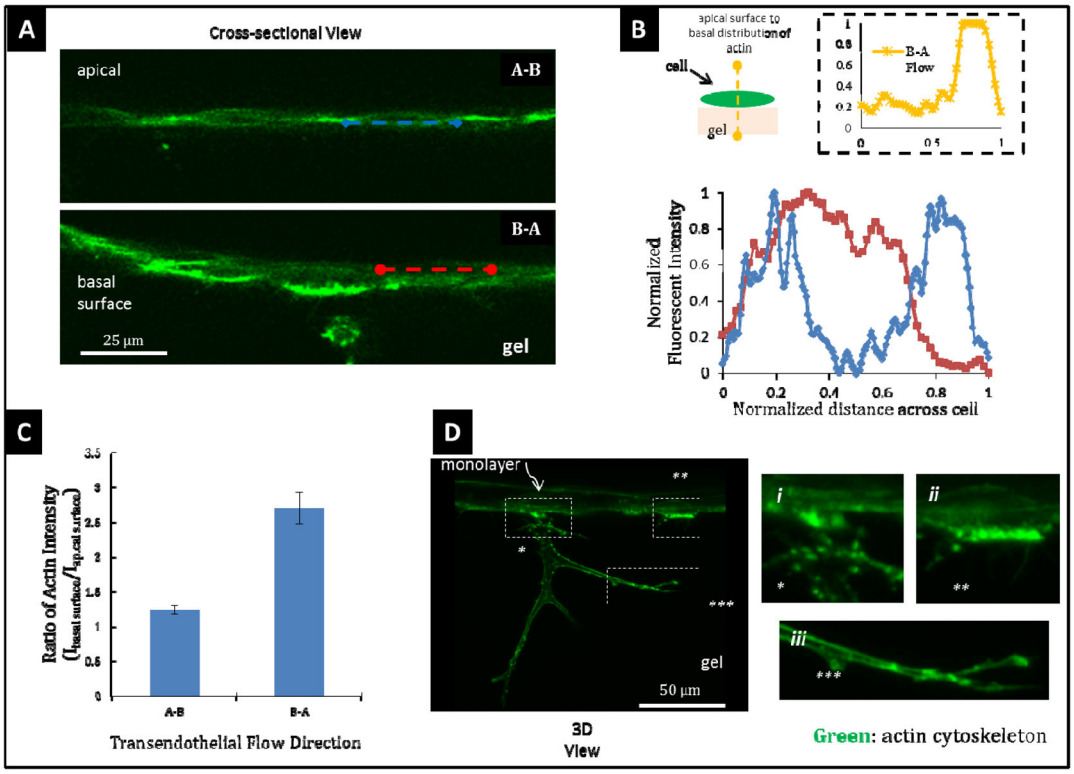

Figure 6.

B-A flow direction affects distribution of cortical actin. (A) Confocal section of HUVEC monolayer exposed to A-B (TOP) and B-A (BOTTOM) flow. Samples were fixed and stained with phalloidin to label actin cytoskeleton. (B) Fluorescent line intensity profile of actin localization across cell for A-B (BLUE) and B-A (RED) flow directions; (INSET) apical surface to basal surface distribution of actin for monolayer subjected to B-A flow, showing notable clustering of actin towards basal surface. (C) Quantification of the impact of flow direction on the degree of actin polarization assessed by the ratio of “basal actin” and “apical actin” intensity. (D) HMVEC, (LEFT) 3D view of a sprouting monolayer stained with phalloidin (RIGHT) Magnification of boxed regions highlighting actin localization and clustering towards basal surfaces.

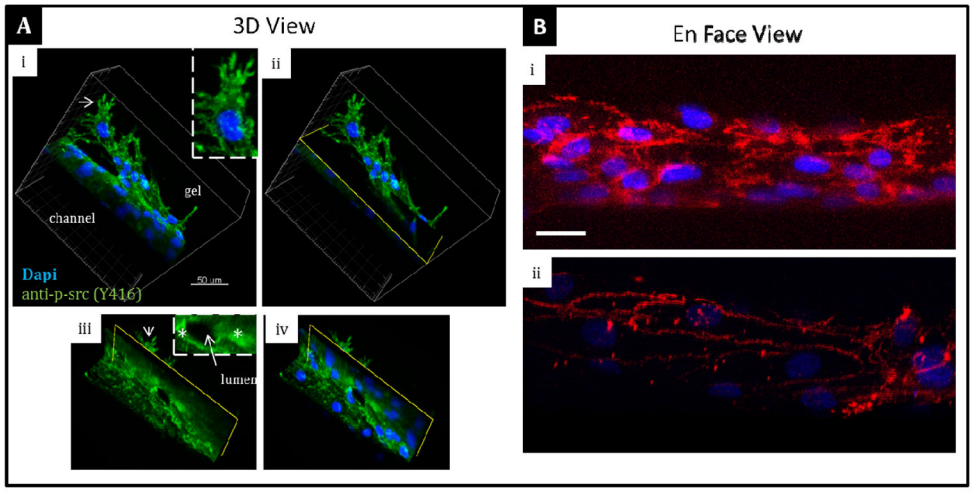

Figure 7.

Src mediates B-A flow induced remodeling at cell-cell junction. (A) Reconstruction of confocal images showing 3D views of B-A flow induced sprouting monolayer stained with anti-p-Src Y416 antibody (GREEN) and DAPI (BLUE). (i–ii) View from basal surface, showing clustering at membrane projections (white arrow) and tip cell (inset); (iii–iv) View from apical surface showing p-Src clustering where sprout emerges from monolayer, around lumen (inset). (B) B-A flow induced VE-cadherin delocalization from junctional complex is mediated by Src. Images show enface view of monolayer subjected to B-A flow (i) without PP2 (control) (ii) with Src inhibitor, PP2 treatment and stained for VE-cadherin (RED) and DAPI (BLUE). Scale bar: 25 μm